World Journal of Radiology

EDITORIAL

Modern imaging of the tracheo-bronchial tree

Archana T Laroia, Brad H Thompson, Sandeep T Laroia, Edwin JR van Beek

Archana T Laroia, Brad H Thompson, Sandeep T Laroia, Edwin JR van Beek, Department of Radiology, University of Iowa Hospitals and Clinics, Iowa City, IA 52241, United States
Edwin JR van Beek, Clinical Research Imaging Centre, Queen's Medical Research Institute, University of Edinburgh, Edinburgh EH16 4TJ, United Kingdom
Author contributions: All authors contributed equally to this manuscript, all supplying images and text.
Correspondence to: Edwin JR van Beek, MD, PhD, MEd, FRCR, SINAPSE Chair of Clinical Radiology, CO.19, Clinical Research Imaging Centre, Queen's Medical Research Institute, University of Edinburgh, 47 Little France Crescent, Edinburgh EH16 4TJ, United Kingdom. edwin-vanbeek@ed.ac.uk
Telephone: +44-131-2427760 Fax: +44-131-2427773
Received: April 15, 2010   Revised: June 9, 2010
Accepted: June 16, 2010
Published online: July 28, 2010

Abstract

Recent state-of-the-art computed tomography and improved three-dimensional (3-D) postprocessing techniques have revolutionized the capability of visualizing airway pathology, offering physicians an advanced view of pathology and allowing for appropriate management planning. This article is a comprehensive review of trachea and main bronchi imaging, with emphasis on the dynamic airway anatomy, and a discussion of a wide variety of diseases including, but not limited to, congenital large airway abnormalities, tracheobronchial stenoses, benign and malignant neoplasms and tracheobronchomalacia. The importance of multiplanar reconstruction, 3-D reconstruction and incorporation of dynamic imaging for non-invasive evaluation of the large airways is stressed.

INTRODUCTION

Imaging of the trachea-bronchial tree has improved recently, in large part due to the advancements of computed tomography (CT), allowing for volumetric isotropic voxel imaging, and its associated improvements in post-processing software that allows for advanced three-dimensional (3-D) visualization. Thus, airway imaging has become a tool that physicians can use to help plan interventional procedures, such as bronchoscopy, stent placement, surgery and subsequent follow-up. It is clear that airway imaging competes with invasive bronchoscopy as a choice in establishing a diagnosis. CT does not offer the chance for biopsy or broncho-alveolar lavage, and also does not allow intervention. This review article is intended to give a broad overview of the disease processes radiologists encounter in daily practice and offers insight into CT imaging protocols.

STRUCTURAL ANATOMY

The trachea is a cartilaginous and fibromuscular conduit for ventilation and bronchial secretions. It extends from the level of C6 (cricoid cartilage) to the carina, approximately located at level of T4-T5, where it bifurcates into left and right main stem bronchi (Figure 1)[1]. In adults, its length, as measured during inspiratory CT, is approximately 11-13 cm, with 2-4 cm being extrathoracic[2]. During inspiration, the trachea is semi-oval in shape with a coronal diameter of 13 to 25 mm in men and 10 to 21 mm in women, and a sagittal diameter of 13 to 27 mm in men and 10 to 23 mm in women. The trachea has 16 to 22 horseshoe bands of cartilage that compose the anterior and lateral walls of the trachea. The posterior tracheal wall lacks cartilage and
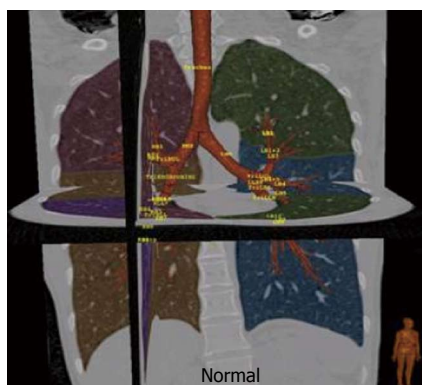
Figure 1 Normal tracheo-bronchial tree with automated lobar segmentation and nomenclature for main airways using dedicated three-dimensional reconstruction software.

is made of a thin membrane supported by the trachealis muscle. On CT, the tracheal wall appears as a 1-3 mm soft tissue stripe outlined by the air in lumen and mediastinal fat. The posterior wall appears thinner and gives a variable contour to the shape of the trachea due to lack of cartilage. It may appear flat, convex or slightly concave depending on the level of inspiration[1,3,4]. The posterior wall of the trachea either flattens or bows slightly forward during expiration. In normal subjects there is up to a 35% reduction in AP tracheal lumen in forced expiration, whereas the transverse diameter decreases only by 13% (Figure 2)[4,5]. The trachea is generally midline in position, often displaced slightly to the right at the level of the aortic arch. It angles posteriorly achieving a mid-coronal location at the level of the carina. Significant error in measurement of the tracheal diameter can occur if the measurement is not perpendicular to the plane of scanning. However, with isotropic imaging made possible with multidetector CT (MDCT), 3-D reconstruction of the airways allows determination of the central axis and hence enables very accurate measurement of the tracheal diameter in any axis. The tracheal index can be calculated as a ratio of the coronal diameter (mm) by the sagittal diameter (mm). The normal value is approximately one[6]. The angle of the tracheal bifurcation, also called the carinal angle, can vary widely even in normal individuals. The carinal angle is wider in individuals with an enlarged left atrium, in females, in obese patients, and in people with the carina located closer to the spine. The widening of the carinal angle on serial films can suggest subcardinal lymphadenopathy. The right main stem bronchus has a more direct downward course, is shorter than the left and begins to ramify earlier than the left main bronchus[1].

IMAGING MODALITIES

The plain chest radiograph is relatively insensitive to airway changes[7]. MDCT, including thin-slice volumetric CT, paired inspiratory and expiratory MDCT and even dynamic 4D MDCT during a full respiratory cycle, allows for exquisite visualization of the central airways. Furthermore, reconstruction methods, including multiplanar imaging and
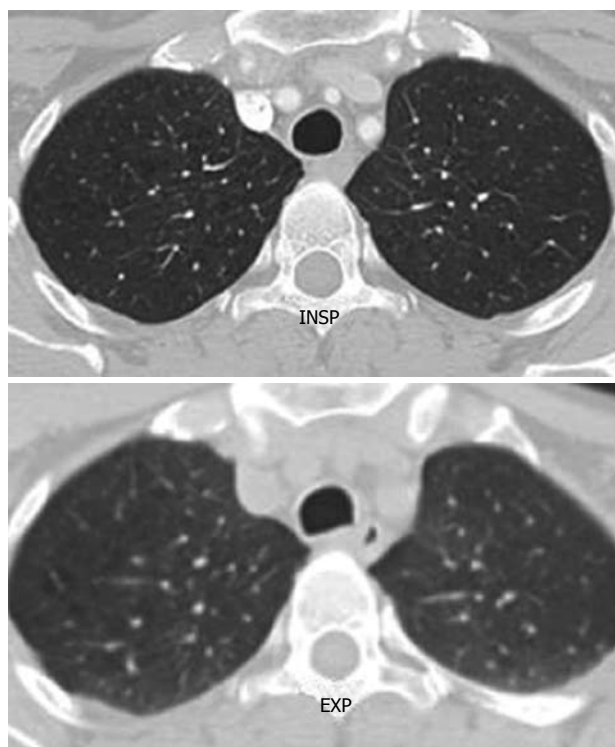

Figure 2 Axial computed tomography image shows the normal rounded configuration of the trachea at the end of inspiration. Note the normal anterior bowing of the posterior membranous wall of the trachea at the end of expiration.

virtual bronchoscopy, are now commonly available. The use of these techniques will be described in greater detail in the sections below, with the most useful techniques highlighted for the various pathologies under evaluation. In addition, MR imaging is increasingly being used to study respiratory dynamics and airway pathophysiology, however, this modality will not be included in this review. Suffice it to say that fast acquisitions of isotropic volumetric data with advanced reconstruction techniques are now capable of generating high quality images with functional information. This has made a significant impact in the direct planning and management of patients[8-11]. Pathology of the trachea and the main stem bronchi can be broadly classified into focal or diffuse causes, with or without tracheabronchomegaly (Table 1).

IMAGE ACQUISTION AND POST PROCESSING

The newer multidetector scanners of 64-128 rows of detector and collimators as thin as 0.625 create a near isometric resolution voxel of 0.4 mm. Slices are reconstructed, with 50% overlap, in the transaxial plane. A rotation time of approximately 500 ms allows a significant decrease in cardiac pulsation artifacts and allows a good analysis of all bronchi, including the paracardiac areas. State-of the-art, 320-detector CT scanners can cover 16 cm of tissue in 350 ms, and hence can image the entire intrathoracic trachea with just a single gantry rotation. This permits dynamic cine imaging of the trachea and bronchi during respiratory maneuvers

Table 1 Broad classification of diseases of the trachea and main-stem bronchi

Diffuse tracheal pathology
  Associated with tracheobronchomegaly
    Related to recurrent chest infections (most common cause)
    Tracheobronchomegaly (Mounier-Kuhn disease)
    Ehlers-Danlos syndrome
    Saber-sheath trachea (increased sagittal diameter)
  Asssociated with a normal or decreased size of the trachea
    Tracheo-bronchomalacia
    Relapsing polychondritis
    Wegener granulomatosis
    Acute tracheo-bronchitis of infectious etiology
    Chronic tracheobronchitis associated with autoimmune diseases
    Tracheal web
    Amyloidosis
    Sarcoidosis
    Tracheopathia osteoplastica
Focal tracheal pathology
  Intrinsic
    Acquired tracheal stricture (mostly iatrogenic related to intubation)
    Idiopathic tracheal stricture
    Benign neoplasms
    Primary malignant neoplasms
    Secondary malignant neoplasms
  Extrinsic
    Compression from adjacent structures or lymphadenopathy
    Vascular anomalies/slings

without significant cardiac or respiratory motion artifacts. The unique inherent natural contrast of the airways and lung parenchyma permits imaging with a relatively lower radiation dose without significant loss of information (100-120 kV, 60-160 mAs). Imaging is obtained in suspended inspiration. Expiratory imaging is obtained to evaluate for tracheomalacia and to evaluate the mosaic perfusion pattern in the lungs to look for small airways disease.

Axial sections with cine mode viewing

Axial images provide detailed evaluation of the size and shape of the airway, wall thickness, presence of calcification, presence of intraluminal lesions, and delineate the relationship of the airways to adjacent mediastinal structures. Evaluation of the thin axial images in a cine mode allows analysis of bronchial divisions to a subsegmental level. Axial imaging can, however, overlook subtle narrowing, so for a comprehensive evaluation of the airways, axial imaging must be complemented with 2-D and 3-D reformation. Multiplanar and 3-D reconstructions enable efficient review of the airways by markedly decreasing the number of images to be evaluated. 2-D and 3-D reformation are more anatomically meaningful formats and, hence, more clinician and patient friendly.

Two-dimensional multiplanar reformation

Two-dimensional multiplanar reformation images are single-voxel-thick sections; 0.6-0.8 mm sections displayed in the coronal, sagittal, or oblique plane. Curved reformations along the long axis of the airways allows for the simultaneous depiction of multiple contiguous airway segments

on a single section. Most PACS stations now permit creation of realtime multiplanar images focusing on the abnormality at the reading workstation itself. A remote post processing station can also be used. Multiplanar reformats are easily performed in real time in all directions with various rendering modes. Multiple adjacent thin slices can be stacked together to generate a thick slab or multiplanar volume reformation image. Slice thickness can be altered to any dimension, but 3 to 7 mm thicknesses generally give adequate images. Various rendering tools can be used. The average MPR can give tomographic equivalent images. Minimum intensity projection (mIP) projects the pixels with the lowest attenuation values in a 2-D format. The trachea-bronchial tree and any lucent abnormalities, such as diverticula or fistulous communications, are well displayed on mIP reconstructions.

3-D reconstruction

3-D reconstructions include external and internal renderings of the airways. External 3-D rendering of the airways is equivalent to CT bronchography. 3-D segmentation of the trachea-bronchial tree provides a rapid anatomic overview of the airways. 3-D reconstructions allow the recognition of mild and focal airway stenoses, providing accurate anatomically more relevant information on the shape, length, and severity of airway stenoses. 3-D images demonstrate the changes of tracheomalacia on inspiration and expiration well.

Internal 3-D rendering of the airways gives images equivalent to bronchoscopy and is aptly referred to as virtual bronchoscopy. It enables the viewer to navigate through the lumen of the airway to the sixth-order and seventh-order subdivisions. Virtual bronchoscopy is a uniquely useful noninvasive method of assessment of tight airway stenosis, which cannot be negotiated on conventional bronchoscopy. It allows for preplanning transbronchial biopsies, evaluation of aspirated foreign bodies and tracheomalacia. Virtual bronchoscopy may obviate the need for invasive conventional bronchoscopy in certain circumstances. It is a great non invasive alternative to conventional bronchoscopy in special subgroups of patients such as young children, very sick patients or elderly patients who may not be able to tolerate bronchoscopy. Virtual bronchoscopy does not permit tissue sampling, which can be done with endoscopic bronchoscopy[12-14].

CONGENITAL TRACHEA-BRONCHIAL ANOMALIES

Bronchus suis

Bronchus suis refers to a rare congenital anomaly, whereby the right upper lobe bronchus originates directly from the trachea (Figure 3). It is usually detected incidentally and may not have much clinical implication. However, this anomaly may cause hypoxemia and prolonged atelectasis with intubation or during anesthesia due to inadvertent closure of the bronchial opening by the endotracheal tube[15-20]. Fur-
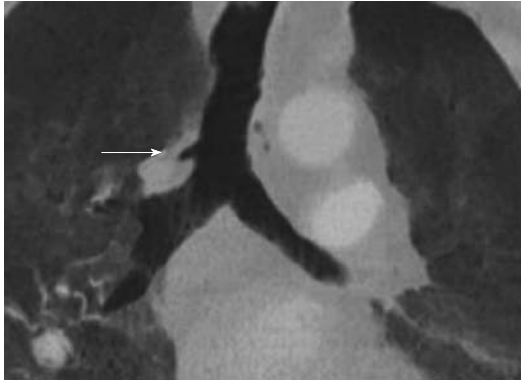
Figure 3 Minimum intensity projection coronal view demonstrating "bronchus suis" (arrow) arising from the right wall of the distal trachea.

thermore, bronchus suis is associated with other congenital anomalies, particularly trisomy 21[21]. Hence, identification of this anomaly is of clinical relevance.

Bronchial atresia

This is a developmental disorder, resulting in a segmental or subsegmental bronchus becoming entirely detached from the main airway[22,23]. The distal airway will continue to produce mucus while there is no clearance from the airway, leading to the impaction of mucus seen as the "finger-in-glove" sign on CT (Figure 4). There is collateral air flow into the segment through the pores of Kohn but it becomes trapped causing hyperinflation of the involved segment. Recurrent pneumonia may be a presenting symptom in these patients. The classic locations for atretic bronchi are the apical and apicoposterior segments of the upper lobes[24].

Tracheo-esophageal fistula

Tracheo-esophageal fistula congenital malformation results from a failure of the trachea and esophagus to divide and grow out separately during early development of the primitive foregut. It is often seen in association with other congenital anomalies, of which the VACTERL is most commonly known[15,25]. VACTERL is a well-known congenital malformation syndrome that includes vertebral, anal, cardiac, tracheoesophageal, renal, and limb anomalies. Esophageal atresia is most commonly proximally positioned with a distal trachea-esophageal fistula (80%-90% of cases), while 5%-8% of fistulas are H-shaped without esophageal atresia[15,26].

DIFFUSE TRACHEAL PATHOLOGY

Dilatation of the trachea may be caused by rare congenital abnormalities, including Mounier Kuhn's disease, Ehlers-Danlos syndrome, or more commonly by chronic acquired conditions with recurrent infections (including those associated with cystic fibrosis, tuberculosis, sarcoidosis and histoplasmosis) and allergic reactions leading to fibrosis of the upper lobes, which affects airflow in the main airways.
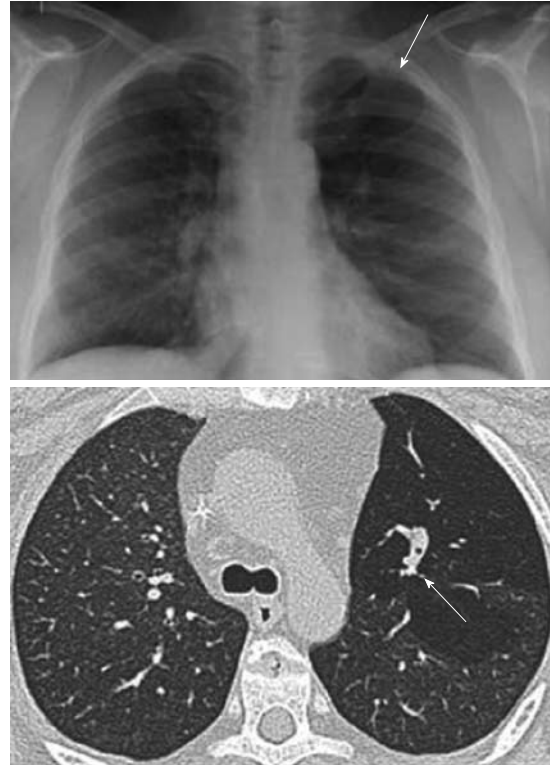

Figure 4 Congenital bronchial atresia. Chest X-ray showing relative lucency of the left upper lobe (arrows). The axial computed tomography section showing hyperinflation in the left upper with non-enhancing branching tubular structure representing the mucus filled left upper lobe bronchus. This appearance is virtually diagnostic of congenital bronchial atresia.

Tracheobronchomegaly (Mounier-kuhn disease)

Tracheobronchomegaly is a rare condition of unknown origin, mainly affecting men in their 4th or 5th decade, however, pediatric patients may also present with this disorder (Figure 5)[27,28]. The process was first described by the French physician Mounier-Kuhn[23] in 1932, and the name was suggested by Katz *et al*[29] in 1962. Approximately 95% of patients are male and there is an autosomal recessive inheritance. In the early stages of this disorder, patients remain asymptomatic or may present with recurrent bronchitis or pneumonia. As the airway disease progresses, air flow obstruction is commonly encountered and repeated infections lead to progressive disability. The process is characterized by dilation of the trachea and main bronchi caused by severe atrophy of longitudinal elastic fibers and thinning of the muscularis mucosa. Tracheomegaly ensues with flaccid, dilated central airways on inspiration with a tracheal diameter greater than 3 cm, whereas on expiration and during coughing the airway collapses (leading to outflow obstruction)[28]. Airway mucosa protrudes through the intracartilaginous skeleton, leading to broad-based diverticula and a corrugated appearance of the trachea on 3-D reconstructions. The diverticula may become extremely pronounced and an interconnected mesh of airway connections may develop with trapped air content. Bronchiectasis and tracheobronchomalacia are commonly associated with this process.
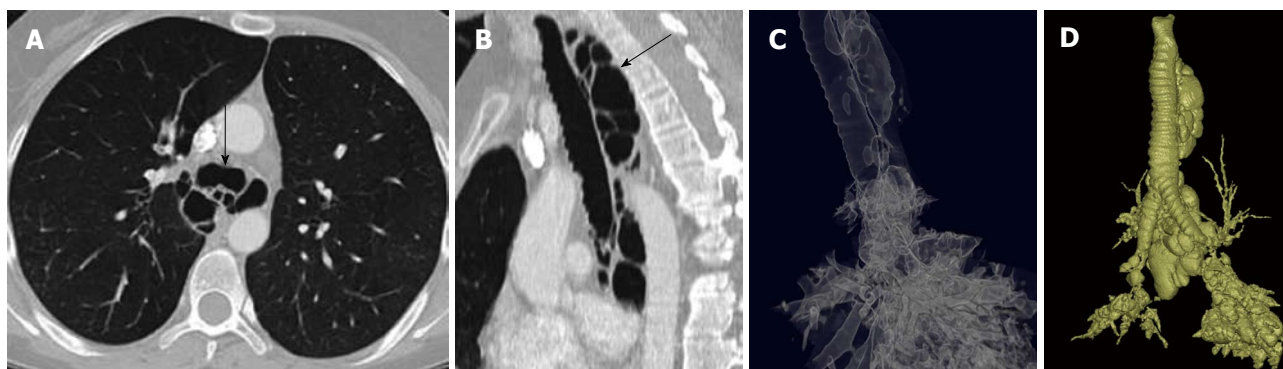
Figure 5 Mounier Kuhn syndrome (congenital tracheobronchomegaly). Axial computed tomography (A), multiplanar sagittal (B) and the minimum intensity projection reconstruction (C) show tracheal enlargement with multiple paratracheal and peribronchial diverticule (arrows). The maximum intensity projection reconstruction (D) demonstrates all interconnected airway structures.
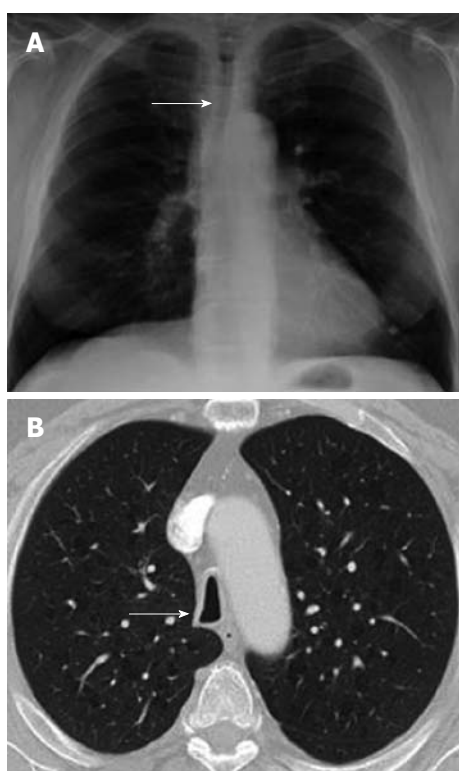

Figure 6 Saber sheath trachea. A: Chest radiograph PA view demonstrating diffuse narrowing of the trachea (arrow); B: Axial computed tomography scan showing inward bowing of the lateral tracheal wall (arrow) with elongated sagittal dimension of the trachea compared to the coronal plane is consistent with the saber sheath configuration.

Saber sheath trachea

Saber sheath trachea is a common condition associated with chronic obstructive pulmonary diseases or advanced age. One study showed a direct correlation between pulmonary outflow obstruction and the extent of the anomaly[30]. It affects the intrathoracic trachea, sparing the cervical trachea. The tracheal wall thickness is normal or mildly increased. The diagnostic term refers to marked coronal narrowing in the presence of accentuation of the sagittal diameter (leading to a sagittal:coronal ratio of greater than 2). Saber-sheath trachea may give rise to unexpected ven-

tilation difficulties if not diagnosed prior to intubation[31]. Chest radiographs may show diffuse narrowing of the trachea on the PA view (Figure 6A). CT shows inward bowing of the lateral tracheal wall, which may be accentuated on the expiratory or dynamic CT, with the classic narrow "saber sheath" shape (Figure 6B)[2].

TRACHEAL AND BRONCHIAL NARROWING

Tracheo-bronchial narrowing is much more common than widening. It can result from a wide variety of causes. MDCT with 3-D reformations from the isotropic data acquisitions allows excellent imaging of the entire trachea-bronchial tree in one breath hold and is capable of demonstrating clinically significant outflow obstruction using inspiration and expiration imaging in combination, as well as the full extent of the disease process with additional applications like cine-CT and virtual bronchoscopy[6,32-34].

Tracheo-bronchial malacia

Tracheo-bronchial malacia is increasingly recognized as one of the more frequent diffuse pathologies in clinical practice. It is most commonly the result of chronic inflammation of the airways associated with chronic obstructive pulmonary disease. Other causes may include inherent weakness of the trachea-bronchial cartilage, such as is seen in osteogenesis imperfecta (a type of primary trachea-bronchial malacia), or relapsing polychondritis (discussed in more detail below). Focal forms of malacia are seen in patients with compression of the trachea due to vascular rings or enlarged goiters. The hallmark of trachea-bronchial malacia is the weakness of the cartilaginous rings, allowing collapse of the posterior membranous wall during expiration, leading to outflow obstruction and airtrapping. The main imaging finding is the variable degree of collapse of the airway during expiration, sometimes with almost complete loss of the airway lumen at the end of expiration resulting in airtrapping. These changes are best observed on combined inspiratory and expiratory CT scans (Figure 7). A "frownlike" tracheal configuration, due to the marked
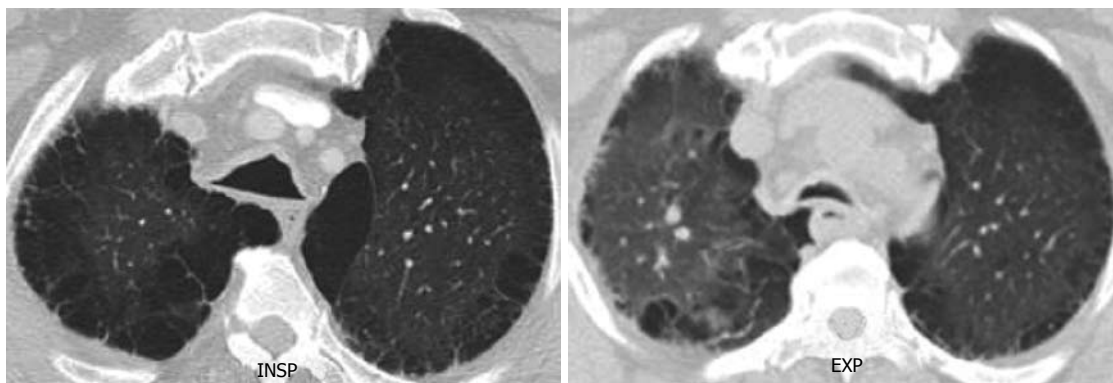
Figure 7 Tracheomalacia. End inspiratory and end expiratory axial computed tomography scan shows excessive collapse of the posterior wall of the trachea in expiration. Note the extensive changes consistent with emphysema in both lungs.
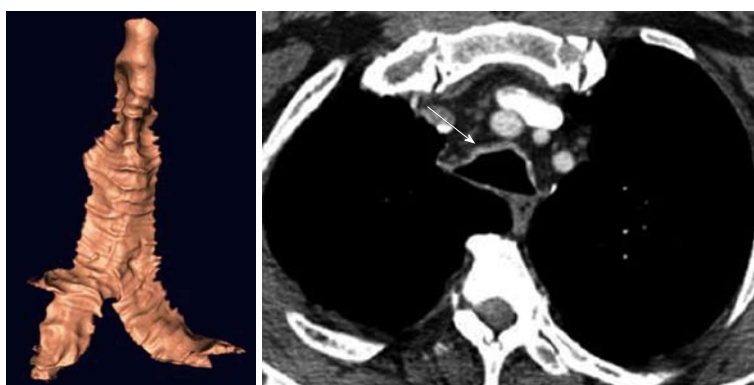

Figure 8 Relapsing polychondritis. Note the characteristic thickening of the anterior cartilaginous wall of the trachea (arrow). The posterior membranous wall is uninvolved.

Figure 9 Subglottic stenosis. Three-dimensional (3-D) shaded surface display computed tomography (CT) image shows smooth focal narrowing of the trachea in the subglottic region (arrow). The extent of the stenosis is much better demonstrated on the 3-D images than on axial CT images.

anterior bowing of the posterior membranous wall forming a crescenteric configuration, has been described as characteristic of tracheomalacia[35-38].

Relapsing polychondritis

Relapsing polychondritis disorder may be caused by a range of etiologies, including vasculitis[39], amyloidosis and infectious processes. However, many patients do not have a clear etiology upon presentation. The cartilaginous part of the airway (extending from the nose to distal conducting airways), the ears and the joints are progressively destroyed due to an autoimmune process of recurrent inflammation. It results in significant airflow obstruction due to collapse of the trachea and main bronchi during expiration. Approximately 30% of patients also have more distal airway involvement[40]. Association with complex immunological conditions, such as a combination of Crohn's disease, relapsing polychondritis and epidermolysis bullosa acquisita have been described in the literature[41]. The clinical relevance of this disease, thus, is not limited to airflow obstruction but extends to systemic involvement, including heart block and vasculitis of both small and larger vessels. Hence, making prompt diagnosis is of great importance[42]. The CT findings often demonstrate varying degrees of tracheal narrowing, often involving multiple segments of the trachea (Figure 8). At expiration, 90% or more patients show signs of collapse (malacia) with or without airtrapping. Calcifications in the airway walls may be seen in approximately 40% of patients[43,44]. CT is particularly useful for the planning of interventional procedures, such as stent placement, and also for follow-up in patients undergoing anti-inflammatory treatment.

Intubation related stenosis

Although relatively infrequent, intubation related tracheal stenosis (Figure 9) is one of the most feared complications, particularly in crash-type intubations and in patients who require prolonged ventilatory support[45]. The etiology is mainly related to direct trauma (which may even cause perforation) or due to pressure ischemia of the airway from

Figure 10 Extrinsic narrowing of the trachea. Axial computed tomography image in the superior mediastinum demonstrating displacement and narrowing of the proximal trachea (arrow) by a large thyroid mass.

the balloon. In either case, there is a combination of necrosis and/or fibrosis, leading to a progressive stenosis that is typically in a subglottic position or in the upper third of the trachea. CT is highly accurate in detecting the extent of such lesions and is, therefore, very useful in treatment planning for stent placement and subsequent follow-up[46-48].

Idiopathic tracheal stenosis
Most causes of benign intrinsic tracheal stenosis are due to mechanical injuries during trauma, intubation or as a result of chronic inflammatory processes. A review of pathological findings involving 63 patients who underwent resection of idiopathic tracheal stenosis showed that a vast majority of these patients suffered from extensive fibrosis and dilatation of mucus glands, whereas the cartilage had a relatively normal structure (in contrast with chondromalacia). All patients were female, 62 cases were subglottic and/or in the upper one-third of the trachea, and 30% of patients had a history of gastroesophageal reflux[49]. CT is currently not able to distinguish between post-traumatic stricture and this type of etiology.

Extrinsic tracheal narrowing
Thyroid cancer may extend both around and into the trachea, causing stenosis or intraluminal tumor extension with airflow obstruction[50]. In addition, large retrosternal benign and malignant goiters and, rarely, traumatic thyroid hemorrhage, can cause tracheal compression (Figure 10)[51,52]. For all of these conditions, CT is a good modality to show the extent of disease and level of obstruction.

Malignant lymphadenopathy is a common feature of lymphoma and primary lung cancer (both small-cell and non-small cell lung cancer), and may give rise to compression and/or invasion of the trachea. In addition, lymphadenopathy from benign etiologies, such as histoplasmosis and tuberculosis may also cause compression of the trachea (Figure 11). However, due to the anatomy of the trachea, clinically significant external compression caused by lymphadenopathy is relatively uncommon.

Pulmonary artery sling is a condition in which the left pulmonary artery arises from the right main pulmonary
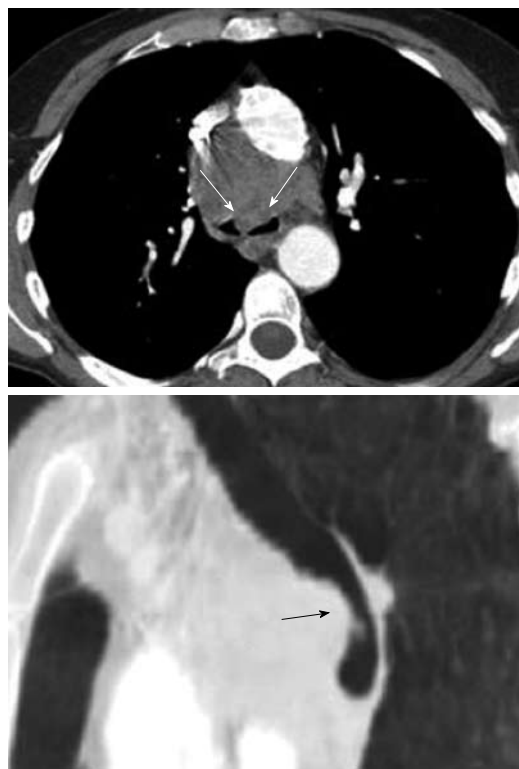

Figure 11 Axial computed tomography image and sagittal multiplanar reconstruction showing invasion of the anterior wall off the carina (arrows) by malignant lymphadenopathy from non-small cell lung cancer.

artery[44]. As the vessel courses to the left lung, it passes between the trachea and esophagus, giving rise to the potential compression of the trachea[53]. Two types exist: Type Ⅰ simply gives rise to posterior compression of the distal trachea and right main stem bronchus with anterior compression on the esophagus, whereas Type Ⅱ is associated with congenital stenosis of the distal trachea, an abnormal low position of the carina and horizontal course of the main bronchi (T-shaped trachea), a bridging bronchus and several other congenital anomalies[54,55]. Both conditions usually become symptomatic in infancy and early childhood and surgical intervention tends to take place early in life. CT is very helpful for delineation of the various pathologies and is also able to detect functional obstruction with airtrapping as demonstrated on expiratory or cine-CT imaging.

A range of other vascular anomalies can give rise to compression of the trachea, including an enlarged brachiocephalic trunk, double aortic arch and aberrant right subclavian artery. CT has proven useful in adequate identification of these anomalies in the pediatric age group[56-58].

Recurrent respiratory papillomatosis
Recurrent respiratory papillomatosis (RRP) is the result of infection of the upper respiratory tract by human papilloma virus types 6 and 11[59]. RRP has a bimodal age distribution, with most infections taking place at birth through an infected birth canal. However, a more aggressive form occurs in young adults. The tracheo-laryngeal form of papillomatosis occurs in 2%-17% cases and eventually spreads to the lungs in 1% of patients.
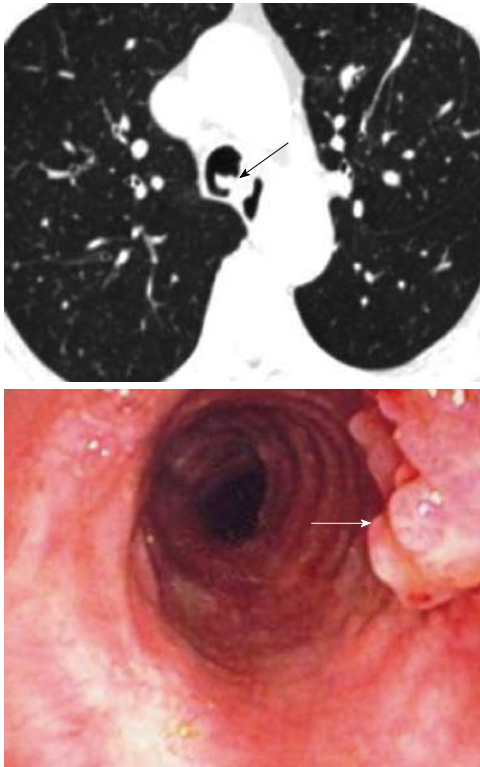
Figure 12 Respiratory papillomatosis. Endoluminal masses in respiratory papillomatosis seen on the axial computed tomography scan (black arrow) and on bronchoscopy (white arrow).
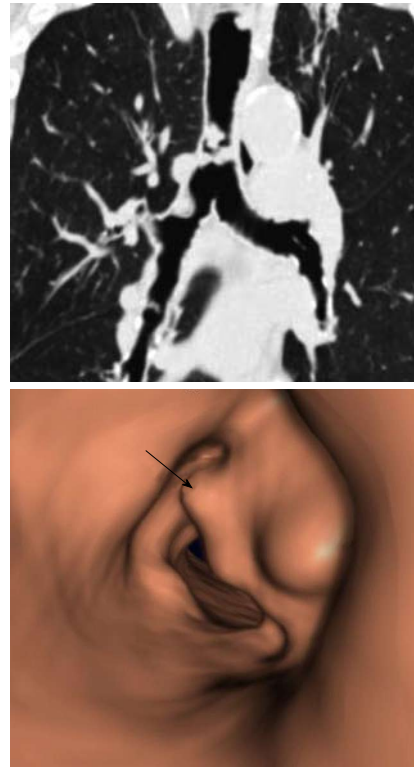

Figure 13 Coronal multiplanar reconstruction and the virtual bronchoscopic image showing extensive involvement of the distal trachea (arrow) and the right bronchus in a case of recurrent respiratory papillomatosis.

RRP is characterized by benign exophytic lesions in the airway, most commonly involving the larynx and central trachea-bronchial tree (Figure 12)[60]. It is postulated that peripheral seeding occurs, particularly when endoscopic or surgical manipulations are necessary to control the central airway patency. However, peripheral lesions may also be the result of multi-centric localization of initial foci of infection. Central lesions tend to grow in similar fashion to the typical papillomas seen externally on the skin. The lesions give rise to tracheal wall irregularities with progressive mass-like protrusions, and airway obstruction may occur (Figure 13). These lesions tend to be well circumscribed and do not give rise to extension beyond the trachea or bronchial wall. Peripheral lesions typically lead to nodules at first, which will grow to a size of 5 to 50 mm and subsequently tend to cavitate with a mixture of thin and thick-walled cavities.

Complications include airway obstruction, atelectasis, pneumonia or pneumothorax. Malignant degeneration to squamous cell carcinoma is the most serious long-term sequel of pulmonary RRP (Figure 14)[61]. The course of the disease is variable, ranging from spontaneous remission to aggressive recurrences requiring multiple surgical procedures in the patient's lifetime and accounts for significant morbidity, poor life quality and higher health care costs. MDCT allows for multiplanar and advance post-processing (including virtual bronchoscopy) and is therefore the preferred modality for noninvasive evaluation of both tracheal and lung lesions. The differential diagnosis of
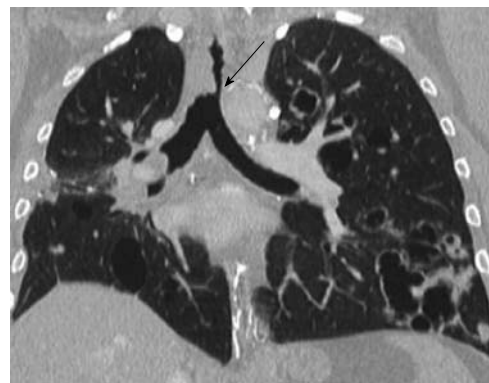

Figure 14 Squamous cell cancer of the trachea (arrow) in a known case of recurrent respiratory papillomatosis. Note the extensive bilateral cystic lung lesions consistent with pulmonary involvement in respiratory papillomatosis.

multiple cavitary nodules includes metastatic tumor, fungal disease, mycobacterial infection, hydatid cyst, septic emboli, rheumatoid nodules, amyloidosis, sarcoidosis, pulmonary angiitis and granulomatosis.

Neoplasms of the trachea

Neoplasms of the trachea are rare, especially when compared to tumors of the lung and mediastinum. In fact, tracheal neoplasms account for less than 1% of all intrathoracic malignancies[7]. The most common malignancy of the central airways is squamous cell carcinoma and adenocystic carcinoma. Only the squamous cell types exhibit
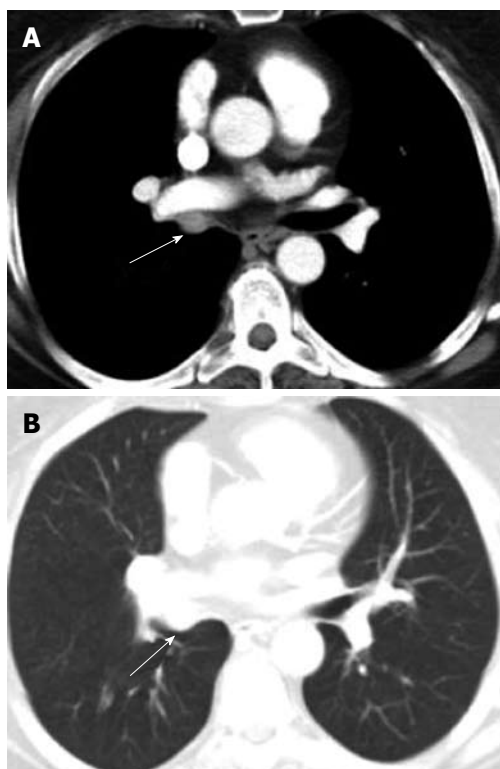
Figure 15 Metastatic melanoma right main bronchus. Axial computed tomography image-mediastinal (A) and lung windows (B) shows enhancing soft tissue mass occupying the right main bronchus (arrows).

Figure 16 Endobronchial hamartoma. Axial computed tomography image (A) and the multiplanar reconstruction in the lung window (B and C) shows chronic bronchiectasis in the left lower lobe (arrow) secondary to a long-standing slow-growing obstruction of the left main bronchus and recurrent infections (arrows).

a link with smoking. A benign counterpart to squamous cell carcinoma, the squamous cell papilloma has also been linked to smokers[62]. Mucoepidermoid and carcinoid tumors are less commonly encountered tumors of the trachea. Metastatic lesions of the trachea and bronchi are most commonly seen with melanoma and breast cancer (Figure 15). Direct tumor invasion into the trachea from adjacent neoplasms originating from lung, esophagus, thyroid and mediastinum are not uncommon. Due to the nonspecific radiographic features characteristic of most endobronchial tumors, the CT appearance is not useful in determining the cell type of most tumors with the exception of hamartomas and lipomas, which contain macroscopic adipose tissue suggestive of their diagnosis (Figure 16). Tracheal neoplasms with internal calcified matrix suggest the diagnosis of chondrosarcoma. Sarcomas of the trachea appear uniformly fleshy (Figure 17). Carcinoid tumors, though generally nonspecific in appearance, may exhibit a higher degree of contrast enhancement than other tracheal neoplasms, which can suggest the diagnosis. MDCT incorporating multiplanar reconstructions is the modality of choice in the evaluation and preoperative planning of tracheal tumors. Dedicated airway studies of the intrathoracic trachea using very thin collimation render exquisite anatomic information that is useful in planning bronchoscopy and surgical resection. CT not only accurately provides location and dimensional information about the tumor, but also provides ancillary information about tumor extension, relationships to adjacent mediastinal structures and airway patency. Furthermore, CT provides
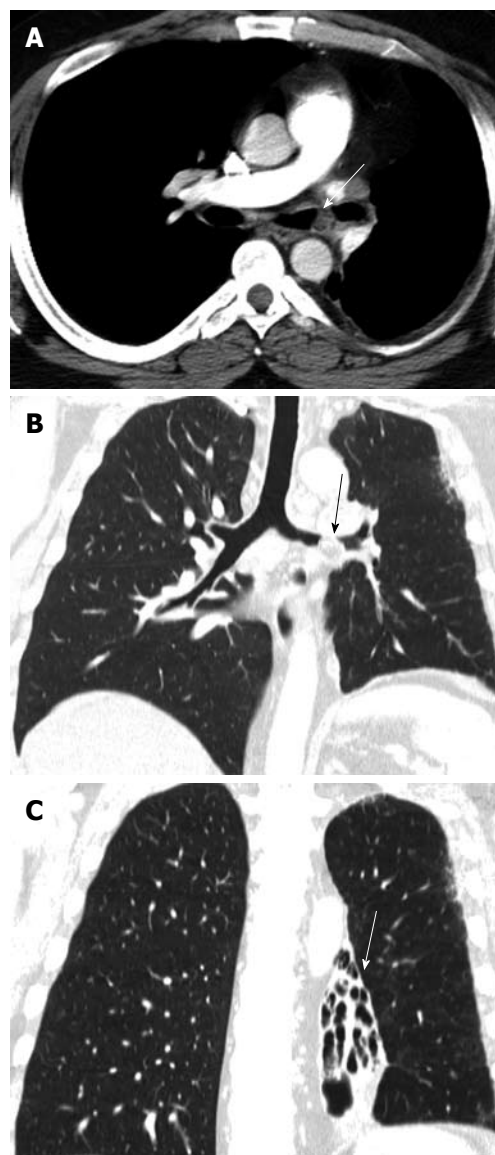
additional information, such as regional lymphadenopathy and pulmonary metastatic disease, which is useful in tumor staging. Virtual bronchoscopy also provides a valuable imaging tool to assess tumor location, size and airway patency complementary to traditional fiberoptic bronchoscopy.

Wegener's granulomatosis

Wegener's granulomatosis (WG) is a systemic vasculitis syndrome characterized by pulmonary angiitis and granulomatosis that can affect any organ in the body, but most commonly involves the kidneys and the sinopulmonary system. The basic pathogenesis of the disease involves small vessel vasculitis. A triad consisting of pulmonary disease, sinusitis and glomerulonephritis are the hallmarks of WG. Although the etiology is unclear, there is some suspicion that the disease may be linked to a potential inhaled infectious agent resulting in a hypersensitivity reac-
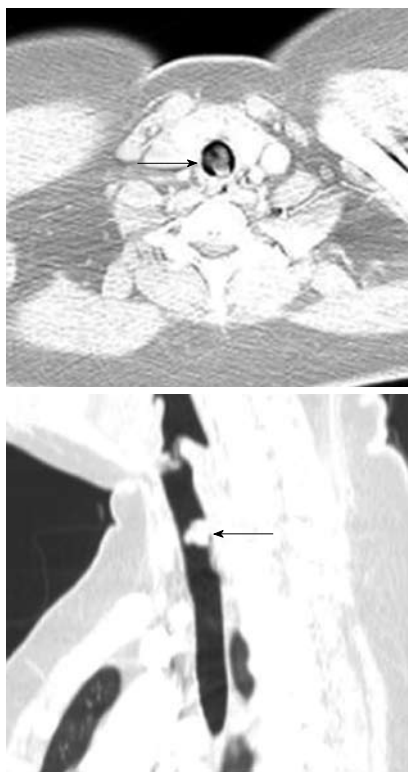
Figure 17 Axial and sagittal reconstruction of the computed tomography scan images demonstrates a fleshy mass within the tracheal lumen (arrows) in a patient presenting with increasing difficulty of breathing. Histopathology following surgical resection demonstrated a primary sarcoma of the trachea.
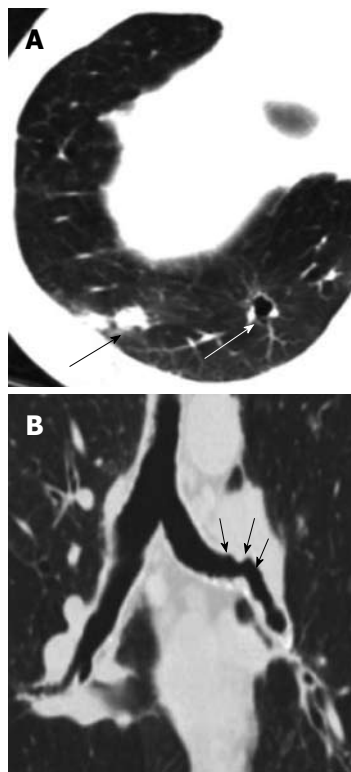

Figure 18 Airway involvement in Wegner's granulomatosis. A: Axial computed tomography image shows cavitary lung nodules (large arrows); B: Coronal multiplanar reconstruction in lung window demonstrates irregular narrowing of the left main bronchus (small arrows).

tion[63]. Serological testing using assays of antineutrophil cytoplasmic autoantibodies (c-ANCA) are instrumental in making the diagnosis[64]. The sensitivity of c-ANCA for WG is 96% for generalized disease and 67% in cases where the disease is more localized. The specificity is 99%[65]. The peak incidence of WG is in the 4th and 5th decades of life with a 3:2 male-female predominance[66,67]. Before the use of immunosuppressive medications, the mean survival of patients with generalized WG was 5 mo from the onset of symptoms, with a 1-year mortality rate of 80%[64]. Fortunately, the survival has been significantly improved with the instigation of combination therapies using cyclophosphamide and corticosteroids, with a mean five-year survival rate now of 90%-95%[63] and a mean survival rate of 21.7 years[64].

Airway involvement in WG is found in 15%-60% of patients but is rarely a presenting feature of the disease for most patients since laryngeal and trachea-bronchial involvements are usually late manifestations of the disease (Figure 18)[68-75]. Bronchoscopic findings include subglottic stenosis, ulcerating tracheobronchitis with or without inflammatory polyps or pseudotumors, and tracheal and bronchial stenosis[67,68].

Subglottic stenosis is the most frequent large airway manifestation of WG occurring in 8.5%-50% of patients[76,77]. Patients with upper airway disease usually present with symptoms of wheezing, stridor or dyspnea reflecting the upper airway lesions associated with WG. Pathologic findings of airway involvement include bronchiolitis, bron-chiolitis obliterans, trachea-bronchial stenosis and destructive chondritis. Multi-detector CT with advanced reconstruction techniques is key in evaluating the trachea-bronchial tree for the characteristic lesions of WG, which may show endobronchial nodules, mucosal thickening and areas of focal or elongated regions of airway stenosis often resulting in areas of post-obstructive atelectasis involvement in WG[78].

CT bronchoscopy has been shown to be useful in depicting these airway abnormalities with good results. Eighty percent of stenotic lesions were detected by CT bronchoscopy in one series[79]. Airway disease, especially sites of stenosis, are commonly fixed and persist despite overall favorable response to treatment in other involved organs.

CONCLUSION

The complementary use of both 2-D and 3-D CT imaging can very accurately define the location as well as intra- and extra-luminal extent of pathology of the central airways. It has become a valuable tool for the clinician to assist with the diagnosis and planning of therapy for both focal and diffuse diseases of the airways. With the currently achieved image quality and versatility of depicting these pathologies, imaging of the airways knows virtually no boundaries.

REFERENCES

1   **Minnich DJ**, Mathisen DJ. Anatomy of the trachea, carina, and bronchi. *Thorac Surg Clin* 2007; **17**: 571-585

2   **Webb EM**, Elicker BM, Webb WR. Using CT to diagnose non-neoplastic tracheal abnormalities: appearance of the tracheal wall. *AJR Am J Roentgenol* 2000; **174**: 1315-1321

3   **Ugalde P**, Miro S, Fréchette E, Deslauriers J. Correlative anatomy for thoracic inlet; glottis and subglottis; trachea, carina, and main bronchi; lobes, fissures, and segments; hilum and pulmonary vascular system; bronchial arteries and lymphatics. *Thorac Surg Clin* 2007; **17**: 639-659

4   **Ederle JR**, Heussel CP, Hast J, Fischer B, Van Beek EJ, Ley S, Thelen M, Kauczor HU. Evaluation of changes in central airway dimensions, lung area and mean lung density at paired inspiratory/expiratory high-resolution computed tomography. *Eur Radiol* 2003; **13**: 2454-2461

5   **Boiselle PM**, Reynolds KF, Ernst A. Multiplanar and three-dimensional imaging of the central airways with multidetector CT. *AJR Am J Roentgenol* 2002; **179**: 301-308

6   **Grenier PA**, Beigelman-Aubry C, Fétita C, Prêteux F, Brauner MW, Lenoir S. New frontiers in CT imaging of airway disease. *Eur Radiol* 2002; **12**: 1022-1044

7   **Kwong JS**, Müller NL, Miller RR. Diseases of the trachea and main-stem bronchi: correlation of CT with pathologic findings. *Radiographics* 1992; **12**: 645-657

8   **Grenier PA**, Beigelman-Aubry C, Fetita C, Martin-Bouyer Y. Multidetector-row CT of the airways. *Semin Roentgenol* 2003; **38**: 146-157

9   **Bauer TL**, Steiner KV. Virtual bronchoscopy: clinical applications and limitations. *Surg Oncol Clin N Am* 2007; **16**: 323-328

10   **Ferguson JS**, McLennan G. Virtual bronchoscopy. *Proc Am Thorac Soc* 2005; **2**: 488-491, 504-505

11   **Finkelstein SE**, Summers RM, Nguyen DM, Schrump DS. Virtual bronchoscopy for evaluation of airway disease. *Thorac Surg Clin* 2004; **14**: 79-86

12   **Lee KS**, Boiselle PM. Update on multidetector computed tomography imaging of the airways. *J Thorac Imaging* 2010; **25**: 112-124

13   **Javidan-Nejad C**. MDCT of trachea and main bronchi. *Radiol Clin North Am* 2010; **48**: 157-176

14   **Beigelman-Aubry C**, Brillet PY, Grenier PA. MDCT of the airways: technique and normal results. *Radiol Clin North Am* 2009; **47**: 185-201

15   **Berrocal T**, Madrid C, Novo S, Gutiérrez J, Arjonilla A, Gómez-León N. Congenital anomalies of the tracheobronchial tree, lung, and mediastinum: embryology, radiology, and pathology. *Radiographics* 2004; **24**: e17

16   **Freeman SJ**, Harvey JE, Goddard PR. Demonstration of supernumerary tracheal bronchus by computed tomographic scanning and magnetic resonance imaging. *Thorax* 1995; **50**: 426-427

17   **Kairamkonda V**, Thorburn K, Sarginson R. Tracheal bronchus associated with VACTERL. *Eur J Pediatr* 2003; **162**: 165-167

18   **Verghese S**, Jensen G, Ratnayaka K, Kanter J. A fluoroscopic diagnosis of bronchus suis or porcine bronchus to explain hypoxemia during anesthesia. *Anesth Analg* 2008; **107**: 1445

19   **Adetayo OA**, Suskind DL. Radiology quiz case: Tracheal bronchus. *Arch Otolaryngol Head Neck Surg* 2006; **132**: 453, 454

20   **O'Sullivan BP**, Frassica JJ, Rayder SM. Tracheal bronchus: a cause of prolonged atelectasis in intubated children. *Chest* 1998; **113**: 537-540

21   **Doolittle AM**, Mair EA. Tracheal bronchus: classification, endoscopic analysis, and airway management. *Otolaryngol Head Neck Surg* 2002; **126**: 240-243

22   **Fraser R**, Colman N, Muller NL, Pare PD. Developmental and metabolic lung disease. In: Fraser R, Colman N, Muller NL, Pare PD, editors. Synopsis of diseases of the chest. 3rd ed. Philadelphia: Elsevier Saunders, 2005: 188-221

23   **Mounier-Kuhn P**. Dilatation de la trachee; constatations radiographiques et bronchoscopiques. *Lyon Med* 1932; **150**: 106-109

24   **Lee EY**, Boiselle PM, Cleveland RH. Multidetector CT evaluation of congenital lung anomalies. *Radiology* 2008; **247**: 632-648

25   **Botto LD**, Khoury MJ, Mastroiacovo P, Castilla EE, Moore CA, Skjaerven R, Mutchinick OM, Borman B, Cocchi G, Czeizel AE, Goujard J, Irgens LM, Lancaster PA, Martínez-Frías ML, Merlob P, Ruusinen A, Stoll C, Sumiyoshi Y. The spectrum of congenital anomalies of the VATER association: an international study. *Am J Med Genet* 1997; **71**: 8-15

26   **Swischuk LE**. Alimentary tract. In: Swischuk LE, editor. Imaging of the newborn, infant, and young child. 5th ed. Philadelphia: Lippincott Williams & Wilkins, 2003: 350-356

27   **Choplin RH**, Wehunt WD, Theros EG. Diffuse lesions of the trachea. *Semin Roentgenol* 1983; **18**: 38-50

28   **Shin MS**, Jackson RM, Ho KJ. Tracheobronchomegaly (Mounier-Kuhn syndrome): CT diagnosis. *AJR Am J Roentgenol* 1988; **150**: 777-779

29   **Katz I**, Levine M, Herman P. Tracheobronchiomegaly. The Mounier-Kuhn syndrome. *Am J Roentgenol Radium Ther Nucl Med* 1962; **88**: 1084-1094

30   **Trigaux JP**, Hermes G, Dubois P, Van Beers B, Delaunois L, Jamart J. CT of saber-sheath trachea. Correlation with clinical, chest radiographic and functional findings. *Acta Radiol* 1994; **35**: 247-250

31   **Garstang JS**, Bailey DM. General anaesthesia in a patient with undiagnosed "saber-sheath" trachea. *Anaesth Intensive Care* 2001; **29**: 417-420

32   **Boiselle PM**, Lee KS, Lin S, Raptopoulos V. Cine CT during coughing for assessment of tracheomalacia: preliminary experience with 64-MDCT. *AJR Am J Roentgenol* 2006; **187**: W175-W177

33   **Boiselle PM**, Lee KS, Ernst A. Multidetector CT of the central airways. *J Thorac Imaging* 2005; **20**: 186-195

34   **Remy-Jardin M**, Remy J, Artaud D, Fribourg M, Duhamel A. Volume rendering of the tracheobronchial tree: clinical evaluation of bronchographic images. *Radiology* 1998; **208**: 761-770

35   **Gilkeson RC**, Ciancibello LM, Hejal RB, Montenegro HD, Lange P. Tracheobronchomalacia: dynamic airway evaluation with multidetector CT. *AJR Am J Roentgenol* 2001; **176**: 205-210

36   **Baroni RH**, Feller-Kopman D, Nishino M, Hatabu H, Loring SH, Ernst A, Boiselle PM. Tracheobronchomalacia: comparison between end-expiratory and dynamic expiratory CT for evaluation of central airway collapse. *Radiology* 2005; **235**: 635-641

37   **Boiselle PM**, Ernst A. Tracheal morphology in patients with tracheomalacia: prevalence of inspiratory lunate and expiratory "frown" shapes. *J Thorac Imaging* 2006; **21**: 190-196

38   **Boiselle PM**, Feller-Kopman D, Ashiku S, Weeks D, Ernst A. Tracheobronchomalacia: evolving role of dynamic multislice helical CT. *Radiol Clin North Am* 2003; **41**: 627-636

39   **Schina M**, Karsaliakos P, Apostolou T, Mousoulis G. Relapsing polychondritis as a secondary phenomenon of primary systemic vasculitis. *Clin Nephrol* 2008; **70**: 446-449

40   **Ernst A**, Rafeq S, Boiselle P, Sung A, Reddy C, Michaud G, Majid A, Herth FJ, Trentham D. Relapsing polychondritis and airway involvement. *Chest* 2009; **135**: 1024-1030

41   **Vicente EF**, Hernández-Núñez A, Aspa J, Aragües M, García-Vicuña R. Crohn's disease, relapsing polychondritis and epidermolysis bullosa acquisita: an immune-mediated inflammatory syndrome. *Rheumatology* (Oxford) 2008; **47**: 380-381

42   **Hojaili B**, Keiser HD. Relapsing polychondritis presenting with complete heart block. *J Clin Rheumatol* 2008; **14**: 24-26

43   **Lee KS**, Ernst A, Trentham DE, Lunn W, Feller-Kopman DJ, Boiselle PM. Relapsing polychondritis: prevalence of expiratory CT airway abnormalities. *Radiology* 2006; **240**: 565-573

44   **Zylak CJ**, Eyler WR, Spizarny DL, Stone CH. Developmental lung anomalies in the adult: radiologic-pathologic correlation. *Radiographics* 2002; **22** Spec No: S25-S43

45   **Sue RD**, Susanto I. Long-term complications of artificial airways. *Clin Chest Med* 2003; **24**: 457-471

46   **Hoppe H**, Dinkel HP, Walder B, von Allmen G, Gugger M, Vock P. Grading airway stenosis down to the segmental level using virtual bronchoscopy. *Chest* 2004; **125**: 704-711

47 **Koletsis EN**, Kalogeropoulou C, Prodromaki E, Kagadis GC, Katsanos K, Spiropoulos K, Petsas T, Nikiforidis GC, Dougenis D. Tumoral and non-tumoral trachea stenoses: evaluation with three-dimensional CT and virtual bronchoscopy. *J Cardiothorac Surg* 2007; **2**: 18

48 **Sun M**, Ernst A, Boiselle PM. MDCT of the central airways: comparison with bronchoscopy in the evaluation of complications of endotracheal and tracheostomy tubes. *J Thorac Imaging* 2007; **22**: 136-142

49 **Mark EJ**, Meng F, Kradin RL, Mathisen DJ, Matsubara O. Idiopathic tracheal stenosis: a clinicopathologic study of 63 cases and comparison of the pathology with chondromalacia. *Am J Surg Pathol* 2008; **32**: 1138-1143

50 **McCaffrey TV**, Bergstralh EJ, Hay ID. Locally invasive papillary thyroid carcinoma: 1940-1990. *Head Neck* 1994; **16**: 165-172

51 **Ket S**, Ozbudak O, Ozdemir T, Dertsiz L. Acute respiratory failure and tracheal obstruction in patients with posterior giant mediastinal (intrathoracic) goiter. *Interact Cardiovasc Thorac Surg* 2004; **3**: 174-175

52 **Oka Y**, Nishijima J, Azuma T, Inada K, Miyazaki S, Nakano H, Nishida Y, Sakata K, Hashimoto J, Izukura M. Blunt thyroid trauma with acute hemorrhage and respiratory distress. *J Emerg Med* 2007; **32**: 381-385

53 **Lee KH**, Yoon CS, Choe KO, Kim MJ, Lee HM, Yoon HK, Kim B. Use of imaging for assessing anatomical relationships of tracheobronchial anomalies associated with left pulmonary artery sling. *Pediatr Radiol* 2001; **31**: 269-278

54 **Berdon WE**. Rings, slings, and other things: vascular compression of the infant trachea updated from the midcentury to the millennium--the legacy of Robert E. Gross, MD, and Edward B. D. Neuhauser, MD. *Radiology* 2000; **216**: 624-632

55 **Lee EY**, Siegel MJ. MDCT of tracheobronchial narrowing in pediatric patients. *J Thorac Imaging* 2007; **22**: 300-309

56 **Katz M**, Konen E, Rozenman J, Szeinberg A, Itzchak Y. Spiral CT and 3D image reconstruction of vascular rings and associated tracheobronchial anomalies. *J Comput Assist Tomogr* 1995; **19**: 564-568

57 **Hopkins KL**, Patrick LE, Simoneaux SF, Bank ER, Parks WJ, Smith SS. Pediatric great vessel anomalies: initial clinical experience with spiral CT angiography. *Radiology* 1996; **200**: 811-815

58 **Honnef D**, Wildberger JE, Das M, Hohl C, Mahnken AH, Barker M, Günther RW, Staatz G. Value of virtual tracheobronchoscopy and bronchography from 16-slice multidetector-row spiral computed tomography for assessment of suspected tracheobronchial stenosis in children. *Eur Radiol* 2006; **16**: 1684-1691

59 **Tasca RA**, Clarke RW. Recurrent respiratory papillomatosis. *Arch Dis Child* 2006; **91**: 689-691

60 **Giménez A**, Franquet T, Prats R, Estrada P, Villalba J, Bagué S. Unusual primary lung tumors: a radiologic-pathologic overview. *Radiographics* 2002; **22**: 601-619

61 **Kozower BD**, Javiden-Nejad C, Lewis JS, Safdar S, Cooper JD, Patterson GA. Clinical-pathologic conference in general thoracic surgery: malignant transformation of recurrent respiratory papillomatosis. *J Thorac Cardiovasc Surg* 2005; **130**: 1190-1193

62 **Grillo HC**, Mathisen DJ. Primary tracheal tumors: treatment and results. *Ann Thorac Surg* 1990; **49**: 69-77

63 **Frazier AA**, Rosado-de-Christenson ML, Galvin JR, Fleming MV. Pulmonary angiitis and granulomatosis: radiologic-pathologic correlation. *Radiographics* 1998; **18**: 687-710; quiz 727

64 **Polychronopoulos VS**, Prakash UB, Golbin JM, Edell ES, Specks U. Airway involvement in Wegener's granulomatosis. *Rheum Dis Clin North Am* 2007; **33**: 755-775, vi

65 **Nölle B**, Specks U, Lüdemann J, Rohrbach MS, DeRemee RA, Gross WL. Anticytoplasmic autoantibodies: their immunodiagnostic value in Wegener granulomatosis. *Ann Intern Med* 1989; **111**: 28-40

66 **Leatherman JW**. The lung in systemic vasculitis. *Semin Respir Infect* 1988; **3**: 274-288

67 **Prince JS**, Duhamel DR, Levin DL, Harrell JH, Friedman PJ. Nonneoplastic lesions of the tracheobronchial wall: radiologic findings with bronchoscopic correlation. *Radiographics* 2002; **22** Spec No: S215-S230

68 **Daum TE**, Specks U, Colby TV, Edell ES, Brutinel MW, Prakash UB, DeRemee RA. Tracheobronchial involvement in Wegener's granulomatosis. *Am J Respir Crit Care Med* 1995; **151**: 522-526

69 **Gluth MB**, Shinners PA, Kasperbauer JL. Subglottic stenosis associated with Wegener's granulomatosis. *Laryngoscope* 2003; **113**: 1304-1307

70 **Cordier JF**, Valeyre D, Guillevin L, Loire R, Brechot JM. Pulmonary Wegener's granulomatosis. A clinical and imaging study of 77 cases. *Chest* 1990; **97**: 906-912

71 **Maguire R**, Fauci AS, Doppman JL, Wolff SM. Unusual radiographic features of Wegener's granulomatosis. *AJR Am J Roentgenol* 1978; **130**: 233-238

72 **Eagleton LE**, Rosher RB, Hawe A, Bilinsky RT. Radiation therapy and mechanical dilation of endobronchial obstruction secondary to Wegener's granulomatosis. *Chest* 1979; **76**: 609-610

73 **Amin R**. Endobronchial involvement in Wegener's granulomatosis. *Postgrad Med J* 1983; **59**: 452-454

74 **Hellmann D**, Laing T, Petri M, Jacobs D, Crumley R, Stulbarg M. Wegener's granulomatosis: isolated involvement of the trachea and larynx. *Ann Rheum Dis* 1987; **46**: 628-631

75 **Travis WD**, Hoffman GS, Leavitt RY, Pass HI, Fauci AS. Surgical pathology of the lung in Wegener's granulomatosis. Review of 87 open lung biopsies from 67 patients. *Am J Surg Pathol* 1991; **15**: 315-333

76 **Langford CA**, Sneller MC, Hallahan CW, Hoffman GS, Kammerer WA, Talar-Williams C, Fauci AS, Lebovics RS. Clinical features and therapeutic management of subglottic stenosis in patients with Wegener's granulomatosis. *Arthritis Rheum* 1996; **39**: 1754-1760

77 **Screaton NJ**, Sivasothy P, Flower CD, Lockwood CM. Tracheal involvement in Wegener's granulomatosis: evaluation using spiral CT. *Clin Radiol* 1998; **53**: 809-815

78 **Mayberry JP**, Primack SL, Müller NL. Thoracic manifestations of systemic autoimmune diseases: radiographic and high-resolution CT findings. *Radiographics* 2000; **20**: 1623-1635

79 **Summers RM**, Aggarwal NR, Sneller MC, Cowan MJ, Wood BJ, Langford CA, Shelhamer JH. CT virtual bronchoscopy of the central airways in patients with Wegener's granulomatosis. *Chest* 2002; **121**: 242-250